Robotica: (2020) volume 38, pp. 1984–2000. © Cambridge University Press 2019
doi:10.1017/S0263574719001772

Multi-Agent Tracking of Non-Holonomic Mobile Robots via Non-Singular Terminal Sliding Mode Control

Bilal M. Yousuf*, Abdul Saboor Khan and Aqib Noor

Department of Electrical, National University of Computer and Emerging Sciences (FAST), Karachi Campus, Karachi, Pakistan
E-mails: aqib.noor@nu.edu.pk, abdul.saboor@nu.edu.pk

(Accepted February 7, 2019. First published online: December 17, 2019)

SUMMARY
This paper deals with the problem of the formation control of nonholonomic mobile robots in the leader–follower scenario without considering the leader information, as a result of its velocity and position. The kinematic model is reformulated as a formation model by incorporating the model uncertainties and external disturbance. The controller is presented in the two-step process. Firstly, the tracking problem is taken into consideration, which can be used as a platform to design a controller for the multi-agents. The proposed controller is designed based on a non-singular fast terminal sliding mode controller (FTSMC), which drives the tracking error to zero in finite time. It not only ensures the tracking but also handles the problem related to non-singularities. Moreover, the design control scheme is modified using high-gain observer to resolve the undefined fluctuations due to man-made errors in sensors. Secondly, the multi-agent tracking problem is considered; hence, a novel formation control is designed using FTSMC, which ensures the formation pattern as well as tracking. Furthermore, the obstacle avoidance algorithm is incorporated to avoid the collision, inside the region of interest. With the Lyapunov analysis, the stability of the proposed algorithm is verified. As a result, simulated graphs are shown to prove the efficacy of the proposed control scheme.

KEYWORDS: Nonholonomic mobile robots; Fast non-singular terminal; Sliding mode control; Trajectory tracking; Lyapunov analysis; High-gain observer

1. Introduction

Over the decade, many researchers have presented the solution for the modern world requirements using advanced technical robots comprises of nonholonomic nature and their respective controllers. They implemented several ideas related to stabilization and tracking depending on the application-oriented control parameters. A robust control algorithm is an approach that explicitly deals with uncertainty. The basic objective of this algorithm is to track down the trajectories in that region where the degree of freedom is more than the number of actuators. In today's world, the mobile robot configuration regarding its mechanical design can be either nonholonomic or holonomic. Holonomic robots are the unidirectional vehicles and they can move toward any path on the configurable space, whereas nonholonomic robots can only move in a particular direction on the configurable space due to its constraints. The design of a controller for a nonholonomic robot is comparatively more convenient in terms of complexity, flexibility to the holonomic one, which is hard to balance out.

The concept of formation control has originated because a single robot cannot perform many delicate tasks likely rescue operations and mapping. With the advancement of these technologies,

* Corresponding author. E-mail: bilal.yousuf@nu.edu.pk

https://doi.org/10.1017/S0263574719001772 Published online by Cambridge University Press

significantly, more automation toward the multi-robotic system has collaborated in the field of transportation. In leader–follower, the leader is the navigator while the followers are intended to follow them. The designed control scheme is used to reduce the tracking error and to improve system performance. The novelty of this paper is to design a simple but robust formation control scheme which stabilizes the robots in a particular pattern as well as reduce the tracking error.

In the recent literature, we have concluded that sliding mode controllers have been used to configure the dynamic nature of the non-linear system which is used for the application of discontinuous control. The capability to handle the model perturbations and external disturbances makes this the most stable controller for mobile robotic applications. In control theory, formation control is still a challenging problem, when it exposed to external disturbance as well as the unknown system dynamics. Some contribution related to the solution to this problem is defined in refs. [1–8]. Guo, Liang, and Li in ref. [1] have addressed the problem of tracking control of mobile robots using a combination technique, which includes a hybrid of back-stepping control combined with the terminal-based sliding mode control. The controller not only tracks the reference signal but also observes the tracking speed. In this regard, another contribution from Asfi et al., in ref. [2], discussed the problem of formation control of wheeled mobile robot. They developed a novel formation control algorithm based on the integral terminal sliding mode control. Furthermore, they add up the obstacle avoidance algorithm to avoid the collision. Zuo, Cui, and Yan in ref. [3] are investigated the formation problem of multiple dynamic systems, which are nonlinear by nature. They design a terminal sliding mode (TSM)-based control using the neighbor robot's information. The proposed algorithm converges the tracking error of each agent toward its neighborhood of the origin in real-time.

Another contribution in ref. [4] addressed the tracking of the electric cylinder, which exposed to uncertainties and external disturbance. The proposed method shows high-velocity tracking precision of the wheel-legged robot application. Bilal et al., ref. [5], discussed the challenges that occur in the tracking of wheeled mobile robots. The proposed controller is designed in two processes. Firstly, they stabilized a single robot at the equilibrium point. Furthermore, they modified the design of the controller to tackle the tracking problem as well. Finally, ref. [7] proposed an adaptive control approach for tracking a mobile robot. Also, they added obstacle avoidance.

This paper addresses the challenges that occur in formation control using non-singular fast terminal sliding mode control (FTSMC). In this paradigm, the multi-agent tracking objective is achieved using a control scheme, though the leader information is not required. It is a significant problem in comparison to the leader–follower formation scenario. The novelty of this paper lies in the designing of a non-singular sliding surface which eliminates the problems defined in the conventional sliding mode control (SMC). Also, it maintains the high-precision tracking transient response. The proposed scheme is designed in a two-step process. Firstly, robust tracking control is designed using fast non-singular sliding mode controller. In reality, the system does not have any sensors attached to measure velocity and position. In this paradigm, we need an algorithm to recover the performance of the state feedback controller. The previous design algorithm is then enhanced with a high-gain observer (HGO). Secondly, the primary model is reformulated as a formation model. For such a system, the designed controller has to assure that the system remains in formation without the assistance of the leader information. As a result, the tracking controller is re-modified by incorporating the FTSMC controller, which eliminates the difficulties caused by the dependent parameters of a continuous state system. Furthermore, the obstacle avoidance algorithm is added to avoid a collision, while maintaining the desired specific pattern. Lyapunov stability is used to verify the performance of the control scheme. The tracking controller efficacy is tested analytically as well as by simulation on both conditions.

The outline of the remaining paper is defined as follows: problem formulation of nonholonomic mobile robot (NMR) is discussed in Section 2. The proposed control algorithm for tracking is presented in Section 3. The problem is addressed again as the formation model and its tracking controller is defined in Section 4, also with its stability analysis and implementation results in different subsections. Lastly, the discussion on the technique with some personal future recommendations is drawn in Section 5.

2. Kinematic System Modeling

This section presents the kinematic model of a wheeled mobile robot as an example. Besides, it has non-integrable constraints as represented in Fig. 1. From the aforementioned statement, the system

https://doi.org/10.1017/S0263574719001772 Published online by Cambridge University Press

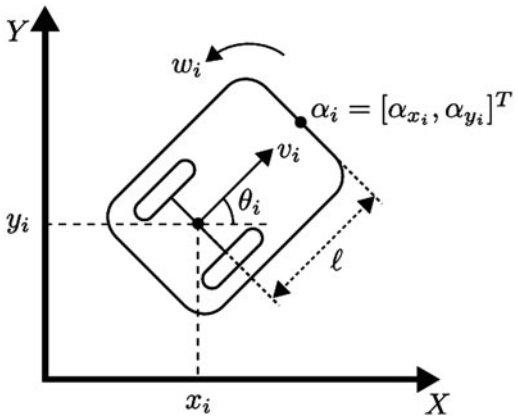


Fig. 1. Kinematic model of nonholonomic mobile robot.[14]

is said to be nonlinear and is moving on X-Y plane. This system is derived based on an assumption of non-slippage and non-friction surfaces. Consider a MIMO system defined as:

$$\dot{p} = \xi(p, u) = S(p)u \tag{1}$$

where $p = [x_o, y_o, \theta_o]$ are the non-integrable constraints, $u = [v, w]$ is the linear and angular velocities, and $S(p)$ is the angular rotation matrix described as:

$$\dot{p} = \begin{bmatrix} \dot{x}_o \\ \dot{y}_o \\ \dot{\theta}_o \end{bmatrix} = \begin{bmatrix} cos\theta_o & 0 \\ sin\theta_o & 0 \\ 0 & 1 \end{bmatrix} \begin{bmatrix} v \\ w \end{bmatrix} = S(p)V \tag{2}$$

Also mentioned earlier that there is no slippage between the wheels and ground. As a result, there will be no friction during the momentum, expressing as:

$$-xsin\theta + ycos\theta = 0$$

where (x_o, y_o) defines as the position of the mobile robot, and θ is the front caster wheel used for heading angle. $(x_o(0), y_o(0), \theta_o(0))^T$ represents the initial values of the system, respectively.

The main outcomes of this paper are presented as follows:

- To design a controller, which tracks down the known reference constant/time-varying trajectories.
- Modify the design of tracking control by incorporating the high-gain observer, to recover the transient performance of the state-feedback controller.
- To design a formation control using FTSMC. Hence, it maintains the desired pattern while tracking the leader without its information.
- To implement the obstacle avoidance algorithm while moving in a particular formation.

3. Designing of Control Algorithm

This section describes the systematic approach to design a robust control scheme for tracking the reference time-varying/constant trajectories for a single mobile robot. For this purpose, a reference model $p_r(t) = [x_r, y_r, \theta_r]$ is considered which indicates the movement of the reference vehicle in Cartesian coordinates as shown in Fig. 2. The design scheme has to follow the reference trajectories written as:

$$\dot{p}_r = \begin{bmatrix} \dot{x}_r \\ \dot{y}_r \\ \dot{\theta}_r \end{bmatrix} = \begin{bmatrix} cos\theta_r & 0 \\ sin\theta_r & 0 \\ 0 & 1 \end{bmatrix} \begin{bmatrix} v_r \\ w_r \end{bmatrix} = S(p_r)V_r \tag{3}$$

x_r, y_r are the position vectors of the reference vehicle, θ_{jr} is the reference heading angle, and v_r, w_r are the reference robot velocities. The proposed design of a control scheme attempts the robot to track

https://doi.org/10.1017/S0263574719001772 Published online by Cambridge University Press

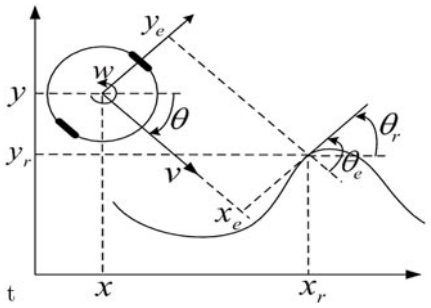


Fig. 2. Reference coordinate of NMR.[15]

it self, and match up the reference trajectory as $t \to \infty, p \to p_r$. For tracking, the system is transformed into a position error model defined as: $p_e = p - p_r - [x_o - x_r, y_o - y_r, \theta_o - \theta_r]$. The change of coordinates of the model can be written as:

$$\begin{bmatrix} e_x \\ e_y \\ e_\theta \end{bmatrix} = \begin{bmatrix} cos\theta_o & sin\theta_o & 0 \\ -sin\theta_o & cos\theta_o & 0 \\ 0 & 0 & 1 \end{bmatrix} * \begin{bmatrix} x_o - x_r \\ y_o - y_r \\ \theta_o - \theta_r \end{bmatrix} \tag{4}$$

Simultaneously taking derivative at both ends of Eq. (4), the equation now can be written as:

$$\dot{p}_e = \begin{bmatrix} \dot{e}_x \\ \dot{e}_y \\ \dot{e}_\theta \end{bmatrix} \begin{bmatrix} we_y + v - v_r cose_\theta \\ -we_x + v_r sine_\theta \\ w - w_r \end{bmatrix} \tag{5}$$

The point to point stabilization of this kinematic model at equilibrium point, mainly origin, can be seen in ref. [5].

3.1. Non-singular tracking control design

In this sub-section, the bounded controller $[v, w]$ is designed to track the position of the reference vehicle in the presence of disturbances. For simplification, we chose the first switching function as $e_x = 0$. To solve the singularity problems, we modify the system dynamics by using a non-singular FTSMC. The sliding surface has a derivative function, which neglects that non-singularities.

Lemma 1. *For all state variables $x \epsilon \Re$ and $|x| < \infty$, there $\varphi(x) = xsin(arctan) \leq 0,'' =''$ come to existence if and only if $x = 0$.*

Theorem 1. *If $\forall\ t \epsilon\ [0, \infty]$, $[v_r, e_y] < \infty$, and all the other reference velocities are bounded, the continuous control scheme Eq. (8) converges the variables e_x and $e_\theta + atan(v_r e_y)$ toward zero in finite time. Therefore, the states x_o and y_o track the desired trajectories in the region of interest.*

Proof: The terminal sliding surface equation can be defined as:

$$\begin{aligned} s_1 &= s_0 + \frac{1}{\Gamma_1} s_0^{\frac{a_1}{b_1}} + \frac{1}{\Gamma_2} \dot{s}_0^{\frac{c_1}{d_1}} \\ s_2 &= s_1 + \frac{1}{\Gamma_1} s_1^{\frac{a_2}{b_2}} + \frac{1}{\Gamma_2} \dot{s}_1^{\frac{c_2}{d_2}} \end{aligned} \tag{6}$$

The terms s_0 and s_1 can be written as:

$$\begin{aligned} s_0 &= e_x \\ s_1 &= e_\theta + atan(v_r e_y) \end{aligned} \tag{7}$$

https://doi.org/10.1017/S0263574719001772 Published online by Cambridge University Press

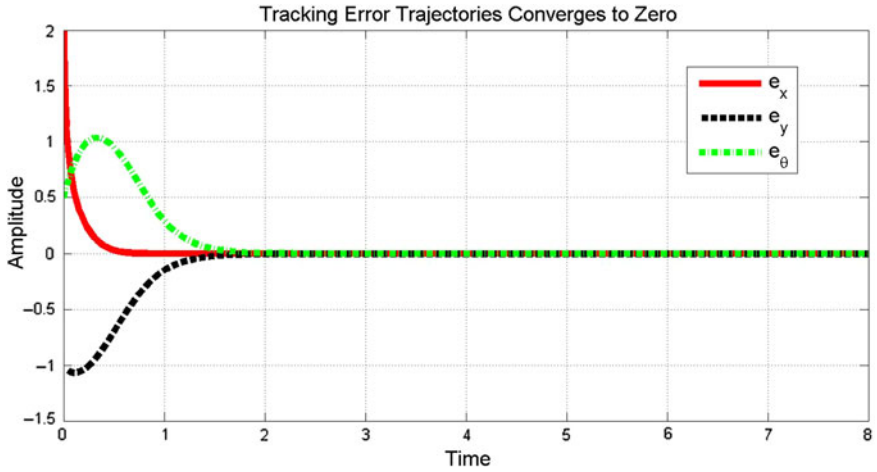


Fig. 3. Tracking error convergence.

In order to define the control equation, substitute Eq. (7) in Eq. (6) using the assumption of $s_2 = 0$. The equation can be written as:

$$v = we_y + v_r cose_\theta \left[+\Gamma_1 \left[e_\theta + arctan(v_r e_y) - e_x - \frac{1}{\Gamma_2} e_x^{\frac{a_1}{b_1}}\right]\right]^{\frac{c_1}{d_1}}$$

$$w = -((1 + v_r^2 e_y^2)\left[-\Gamma_1 \left[e_\theta + arctan(v_r e_y)\right] - \frac{1}{\Gamma_2}(e_\theta + atan(v_r e_y))^{\frac{a_2}{b_2}}\right]^{\frac{c_2}{d_2}} + w_r(1 + v_r^2 e_y^2) + \dot{v}_r e_y + v_r sine_\theta) \div ((1 + v_r^2 e_y^2 + v_r e_x)) \tag{8}$$

Remark 1. Thus, the system equations e_x, e_θ and $arctan(v_r e_y)$ are converged toward zero in finite time using the control Eq. (8). Moreover, it converges much quickly and handles the disturbance more robustly due to the non-singular terminal sliding surface. Furthermore, it has exponent power, so the decay response of the system becomes more reliable, accurate, and it improves the tracking transient response.

3.1.1. Stability analysis. This section discusses the performance of the controller through Lyapunov function. We choose the first switching surface as $e_x = 0$, and the other one can be defined as $V = \frac{1}{2} e_{jy}^2$. Taking the derivative on both sides, now the equation can be written as:

$$\begin{aligned} \dot{V} &= e_y \dot{e}_y \\ \dot{V} &= e_y[-we_x + v_r sine_\theta] \\ \dot{V} &= -e_x e_y w - v_r e_y sin(atan(v_r e_y)) \end{aligned} \tag{9}$$

where $e_{j\theta} = sin(atan(v_r e_y))$ chose as a switching function; hence, using the property of Lemma: 1, we conclude that $v_r e_y sin[arctan(v_r ey)] \leq 0$, if $(v_r e_y = 0)$, as a result of this, this Lyapunov function is going to be negative definite $(\dot{V} \leq 0)$ in finite time.

3.1.2. Simulation results. This section presents the simulated results and discussed the efficacy of the proposed non-singular FTSMC to track the sinusoidal time-varying trajectories. The tracking controller is simulated on MATLAB 17. The selected parameters for simulation are: $\Gamma_1, \Gamma_2 = 6$, $a = 7$, $b = 5$, $c = 11$, $d = 3$. The sinusoidal reference trajectory can be obtained by the following equation:

$$v_r(t) = t, \quad w_r(t) = sin(t). \tag{10}$$

The initial position of vehicle is set for $p_1 = [2, -1, 0.5]$. Figure 3 shows the convergence of the position tracking error in finite time. The tracking error converges toward zero in very less time as

https://doi.org/10.1017/S0263574719001772 Published online by Cambridge University Press

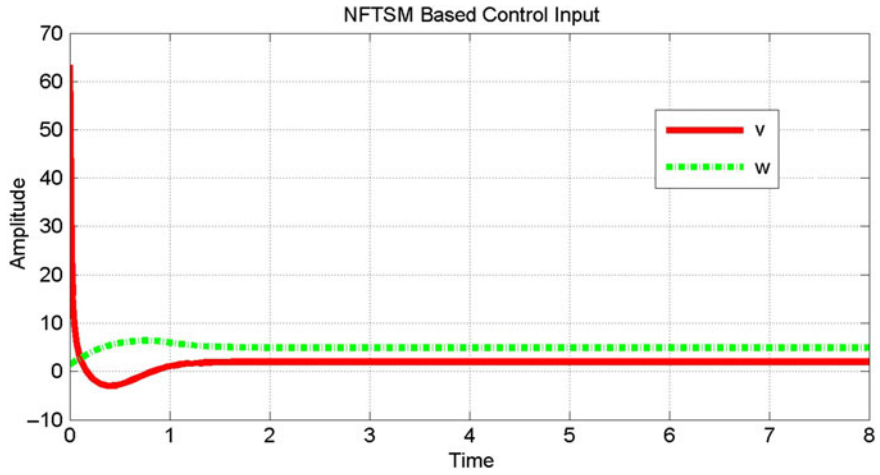


Fig. 4. Non-singular fast terminal sliding mode control inputs.

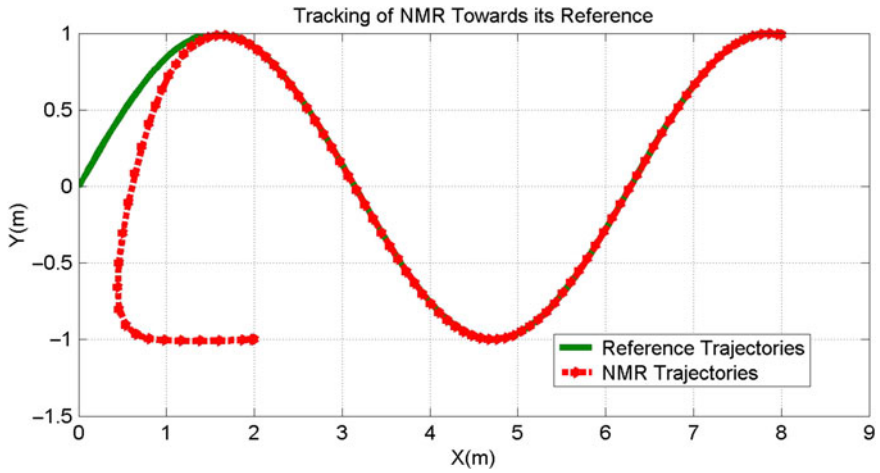


Fig. 5. NMR trajectory tracking in X-Y plane.

compared to other prescribed algorithms.[5] The performance of the control velocities can be seen in Fig. 4. The graph shows how well it matches up with the reference trajectories in an unknown environment. The momentum of the original system can be easily observed in Fig. 5. Furthermore, it proved the efficiency of the desired controller, as it is achieved the tracking objective in less time. The convergence of the sliding surface is visible in Fig. 6. Based on the results, the motion of NMR is well in alignment with the reference velocities, generating the tracking error continuously. The NMR tracks the reference trajectories far better using non-singular FTSMC in comparison to conventional SMC. On the other hand when compared with the conventional one, it shows a better and more robust terms of tracking, and also solves the singularities which might fluctuate the desired results. Moreover, compared with the other papers mentioned in refs. [1, 3, 5], the proposed controller provides better accuracy in transient responses. The real-time decay of tracking error to zero is happening in just 1.15 s, which is more robust as well as quick response compared to ref. [5].

3.2. Modified version of control scheme

This nonholonomic system model does not have the options of placing particular sensors because it will increase the cost as well as the weight of the robots, so the better approach can propagate a controller that can estimate the continuous state, rather being emphasized on the measured ones. For this problem, we incorporated the high-gain observer with the state feedback controller for the estimation of states and also recover the performance of the designed controller. We can reformulate the model in terms of an observer form as:

https://doi.org/10.1017/S0263574719001772 Published online by Cambridge University Press

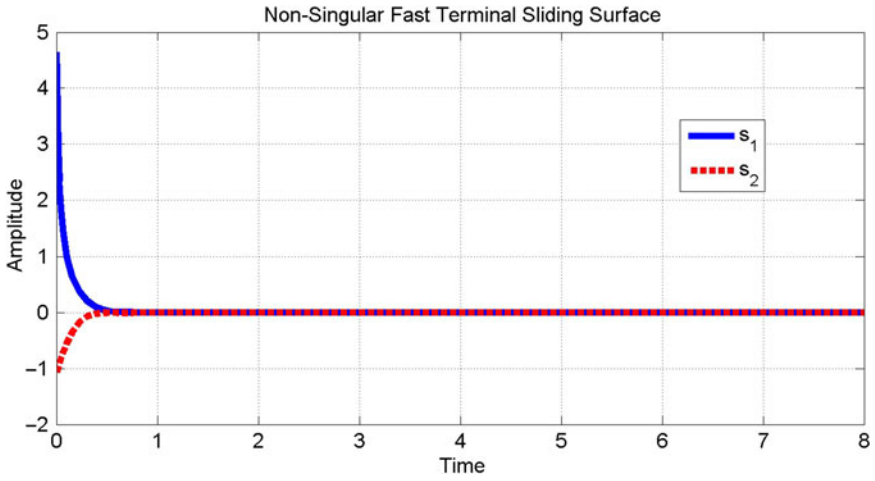


Fig. 6. Non-singular sliding surface.

$$\begin{aligned}
\dot{\hat{e}}_x &= w\hat{e}_y + v - v_r cos\hat{e}_\theta + k_1(e_x - \hat{e}_x) \\
\dot{\hat{e}}_y &= -w\hat{e}_x + v_r sin\hat{e}_\theta + k_2(e_y - \hat{e}_y) \\
\dot{\hat{e}}_\theta &= w + -w_r + k_3(e_\theta - \hat{e}_\theta)
\end{aligned} \tag{11}$$

The HGO-based model can be written as:

$$\begin{aligned}
\tilde{e}_x &= e_x - \hat{e}_x \\
\tilde{e}_y &= e_y - \hat{e}_y \\
\tilde{e}_\theta &= e_\theta - \hat{e}_\theta
\end{aligned} \tag{12}$$

Taking the derivative of Eq. (12), and substitute Eqs. (5) and (11) in Eq. (12), the resultant equation can be written as:

$$\begin{aligned}
\dot{\tilde{e}}_x &= w\tilde{e}_y - v_r cos\tilde{e}_\theta + \frac{h_1}{\epsilon}\tilde{e}_x \\
\dot{\tilde{e}}_y &= -w\tilde{e}_x + v_r sin\tilde{e}_\theta + \frac{h_2}{\epsilon}\tilde{e}_y \\
\dot{\tilde{e}}_\theta &= \frac{h_3}{\epsilon}\tilde{e}_\theta
\end{aligned} \tag{13}$$

$h_i = [h_{1,2}..]$ are the respective gains, and ϵ is the required design parameter, which is needed to reduce the chattering effect.[8] It shows that the HGO-based control Eq. (14) can recover the desired performance of the non-singular FTSMC-based control Eq. (8), by selecting the required design parameters. The output feedback control equation can be written as:

$$\begin{aligned}
v &= w\tilde{e}_y + v_r cos\tilde{e}_\theta \left[+\Gamma_1 \left[\tilde{e}_\theta + arctan(v_r\tilde{e}_y) - \tilde{e}_x - \frac{1}{\Gamma_2}\tilde{e}_x^{\frac{a_1}{b_1}}\right]\right]^{\frac{c_1}{d_1}} \\
w &= -((1 + v_r^2\tilde{e}_y^2)\left[-\Gamma_1[\tilde{e}_\theta + arctan(v_r\tilde{e}_y)] - \frac{1}{\Gamma_2}(\tilde{e}_\theta + atan(v_r\tilde{e}_y))^{\frac{a_2}{b_2}}\right]^{\frac{c_2}{d_2}} + w_r(1 + v_r^2\tilde{e}_y^2) + \dot{v}_r\tilde{e}_y \\
&\quad + v_r sin\tilde{e}_\theta) \div ((1 + v_r^2\tilde{e}_y^2 + v_r\tilde{e}_x))
\end{aligned} \tag{14}$$

3.2.1. Simulation. This section shows the graphical results based on the output feedback control scheme. A sinusoidal trajectory is used to show the effectiveness of the desired approach. The initial

https://doi.org/10.1017/S0263574719001772 Published online by Cambridge University Press

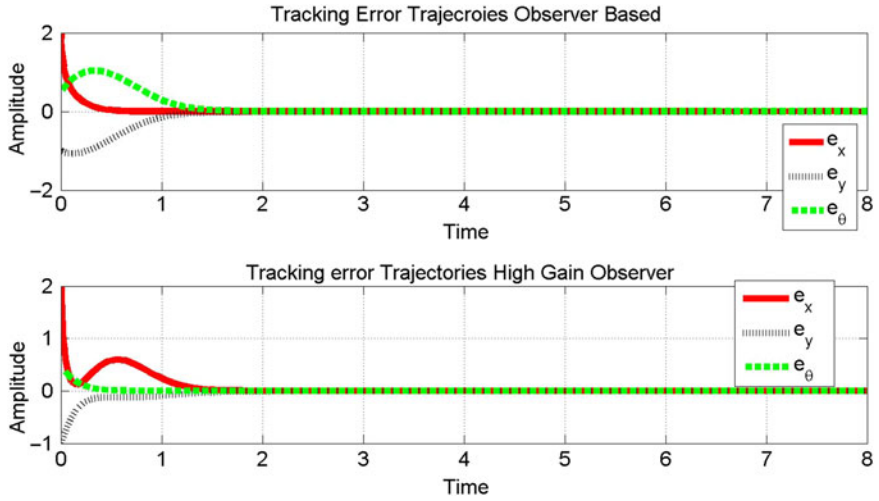


Fig. 7. Tracking error convergence using observer/high-gain observer.

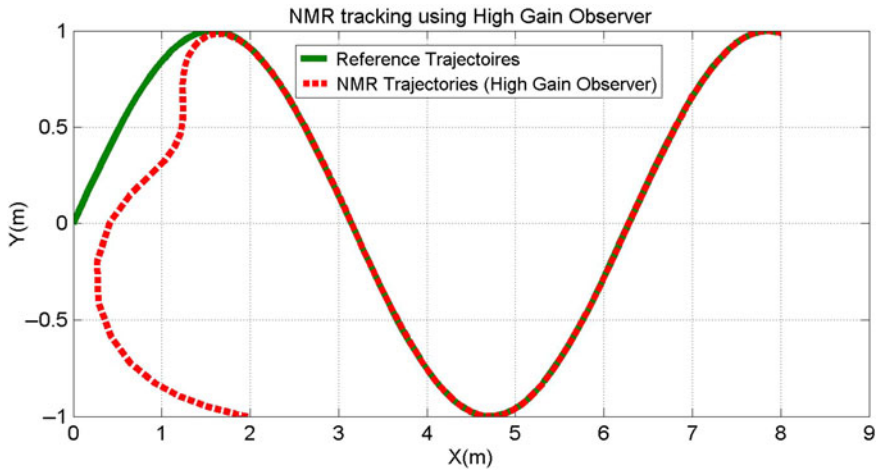


Fig. 8. NMR trajectory tracking in X-Y plane using HGO.

conditions of the NMR are the same as for the state feedback controller. The attainment gains used for this simulation are set as $k_1 = k_2 = k_3 = k_i = 6$, and h_i , $i \epsilon [1, 3]$ are set using $h_i = 10$. Figure 7 shows the tracking error trajectories convergence. As a result, it is more convenient, and robust against disturbance due to fewer perturbations. Figure 8 shows the graphical representation of the controller tracking performance in terms of output feedback control. Figure 9 shows the comparison between the state feedback and output feedback control scheme. It proved that observer-based control recovers the transient performance of the state feedback control in the region of interest.

4. Formation Model

A trajectory tracking of time-varying and constant reference trajectories with the proposed controller is simulated and discussed in earlier sections. Particularly, in this section, we design a novel method based on FTSMC; hence, it verified through simulations. Once the tracking is achieved, the main problem is the involvement of multi-agent formation, which is shown in Fig. 10. Consider N mobile robots, one is the virtual leader and the rest is its followers. The proposed controller will ensure the tracking in rigid structures. The kinematic model for multi-agent NMR $p_j(t)$ can be written as:

$$\dot{p}_j = \begin{bmatrix} \dot{x}_j \\ \dot{y}_j \\ \dot{\theta}_j \end{bmatrix} = \begin{bmatrix} cos\theta_j & -dsin\theta_j \\ sin\theta_o & -dcos\theta_j \\ 0 & 1 \end{bmatrix} \begin{bmatrix} v_j \\ w_j \end{bmatrix} = J(p_j)V_j \tag{15}$$

https://doi.org/10.1017/S0263574719001772 Published online by Cambridge University Press

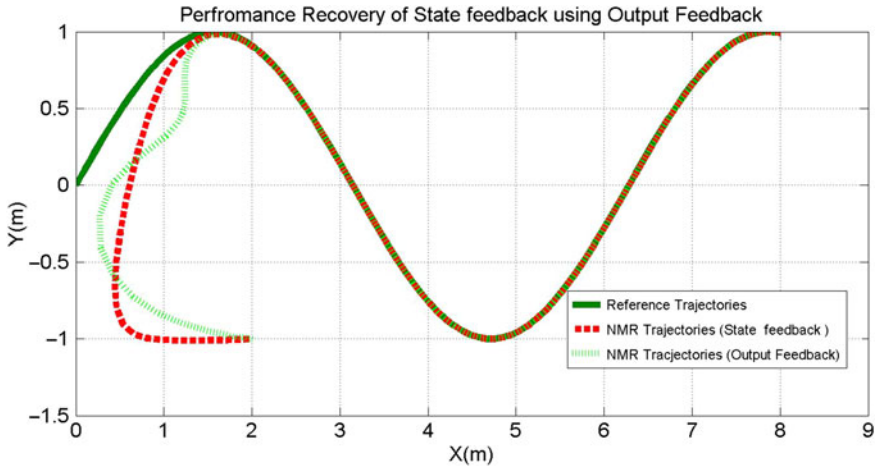


Fig. 9. Performance recovery of state feedback controller using HGO.

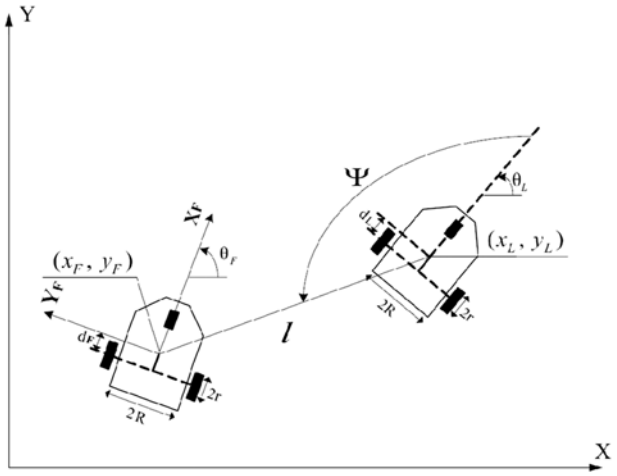


Fig. 10. Formation model of nonholonomic mobile robot.

where j subscript represents the follower robots, and d represents offset distance between the center mass of the robots.

Assumption 1. *For each $j \in N$, there is a separation distance between the center of mass of the followers to the center of mass of the leader L_{oj} such that:*

$$\left|d_{oj}\right| \leq L_{oj} \tag{16}$$

4.1. Graph theory

To solve the problem of communication in mobile robotics, each robot assumes as a node **n** and its communication is denoted through a directed graph such as $G = (V, E, a_{ij})$. v is defined as a set of vertices, E is the subset of vertices denoted as edge, and a_{ij} is denoted as the weighted adjacency matrix of graph G. a_{ij} describe the flow of the states. Node 0 is set as a leader or an exogenous signal which is used as a reference model. If there any edge between o and j, that is, $(v_o, v_j) = \mathrm{E}$, then $a_{oj} > 0$. If there is no edge between the leader and follower, then $a_{ij} = 0$. However, $a_{00} = 0$ for all $o \in N$. The basic idea is to use the neighbor's information, to design a controller that maintains the formation pattern while tracking the leader, and to reach the desired target. The degout of v_j is defined as $deg_{out} = \sum_{j \in N} a_{ij}$. In this paper, we assume that the reference is the leader robot, and the connection between the leader and follower robots is directed.

https://doi.org/10.1017/S0263574719001772 Published online by Cambridge University Press

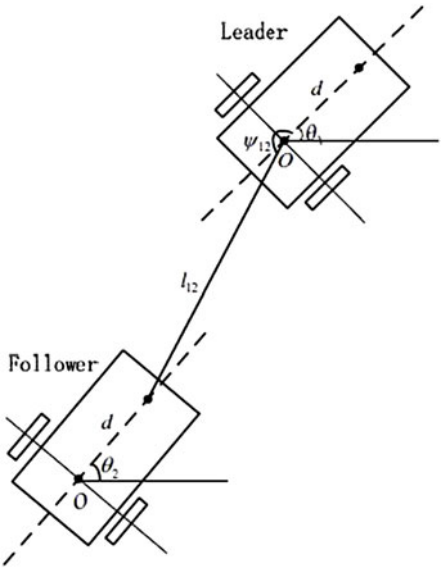


Fig. 11. L-φ formation model.

4.2. $L-\varphi$ formation

Assumption 2. *To handle the formation of robots communication, the possible interaction topologies, $g_\sigma(t)$, for the **n** follower are directed.*

For the re-formulation of N robots, it is necessary to determine a category to coordinate them. The category which is followed in this paper is the leader–follower. Without loss of generality, the o^{th} robot is the leader and others are the follower robot indexing as j^{th} robots. The leader navigates the path for the followers. The follower just follows the path, while maintaining the desired separation distance and bearing angle. Figure 11 defines the relationship of separation and bearing angle between leader and followers. The novelty of this paper is to design a suitable control scheme which deals with the presence of uncertainties.

Assumption 3. *The angular velocities are bounded over finite time as mentioned in the following equation:*

$$-w_{max} \le w_j \le w_{max} \text{ where } w_{max} \text{ is a positive constant}$$

The goal is to design a controller that makes the followers track the leader, although maintaining the separation distance L_{ij}^d and bearing angle φ_{oj}^d. The initial conditions $\varsigma_{oj}^0 = [L_{oj}^0, \varphi_{oj}^0]^T$ are there, such that:

$$\lim_{t\to\infty} = \left\| e_{oj}(t) \right\| = \lim_{t\to\infty} \left\| \begin{bmatrix} L_{oj}^d \\ \varphi_{oj}^d \end{bmatrix} - \begin{bmatrix} L_{oj} \\ \varphi_{oj} \end{bmatrix} \right\| = \lim_{t\to\infty} \left\| \varsigma_{oj}^d - \varsigma_{oj} \right\| \tag{17}$$

$$\lim_{t\to\infty} = \left\| e_{oj}(t) \right\| = \lim_{t\to\infty} \left\| \varsigma_{oj}^d - \varsigma_{oj} \right\|$$

where e_{oj} is the tracking error between the leader and followers $(o-j)$ robots. ς_{oj}^d, ς_{oj} are the desired and actual states, respectively. The actual leader posture with respect to followers can be obtained as

$$\begin{aligned} p_j^d &= [x_j^d, y_j^d, \theta_j^d] \\ &= \begin{bmatrix} x_o - d\cos\theta_j^d + L_{oj}^d \cos(\varphi_{oj}^d + \theta_j^d) \\ x_o - d\sin\theta_j^d + L_{oj}^d \sin(\varphi_{oj}^d + \theta_j^d) \\ \theta_j^d \end{bmatrix} \end{aligned} \tag{18}$$

https://doi.org/10.1017/S0263574719001772 Published online by Cambridge University Press

The derivatives of relative separation distance in Cartesian coordinates $L_{oj}^{x}(t)$, L_{oj}^{y} *can be written as:*

$$\dot{L}_{oj}^{x} = v_0 cos\theta_0 - v_j cos\theta_j + dw_j sin\theta_j$$

$$\dot{L}_{oj}^{y} = v_0 sin\theta_0 - v_j sin\theta_j + dw_j sin\theta_j$$

The relationship of bearing angle between the robots can be defined with the help of the following equation as:

$$\varphi_{oj} = \pi + \varrho_{oj} + \theta_o \tag{19}$$

where ϱ_{oj} *is defined as* $\dfrac{tan^{-1}(y_o y_j - rsin\theta_j)}{x_o - x_j - rcos\theta_j}$, *then the following error model can now be obtained as mentioned in ref. [2]*

$$\begin{bmatrix} \dot{e}_x \\ \dot{e}_y \end{bmatrix} = \begin{bmatrix} cos\psi & -L_{oj}^{d} sin(\varphi_{oj}^{d} + \psi \\ -sin\psi & L_{oj}^{d} cos(\varphi_{oj}^{d} + \psi \end{bmatrix} \begin{bmatrix} v_o \\ w_o \end{bmatrix} + \begin{bmatrix} -1 & e_y \\ 0 & -e_x - d \end{bmatrix} \begin{bmatrix} v_j \\ w_j \end{bmatrix} \tag{20}$$

$$\dot{\varsigma}_{oj} = G(e_x, e_y)V_o + T(e_x, e_y)V_{jequ} \tag{21}$$

where $G(e_x, e_y V_o$ *and* $T(e_x, e_y)$ *are formulated as:*

$$G(e_x, e_y) = \begin{bmatrix} v_o cos\psi & -L_{oj}^{d} w_o sin(\varphi_{oj}^{d} + \psi) \\ v_o sin\psi & L_{oj}^{d} w_o cos(\varphi_{oj}^{d} + \psi) \end{bmatrix} \text{ and } T(e_x, e_y) = \begin{bmatrix} -1 & e_y \\ 0 & -e_x - d \end{bmatrix} \tag{22}$$

$\psi = \theta_o - \theta_j$ *is the relative orientation distance between o–j robots.*

Assumption 4. *The reference trajectories are smooth and friction less, defined as:*

$$|e_\theta| \neq \frac{\pi}{2}, \alpha - e_\theta \neq \frac{\pi}{2}$$

where e_θ *is the orientation error between leader and follower, and* α *is the sliding literal angle. Moreover, the major problem is to control the orientation angle, as it always changes while the robot is turning. To solve this, we must consider the desired posture angle as:*

$$\theta_j^d = (v_o sin\psi + L_{oj}^{d} cos(\varphi_{oj}^{d} + \psi) + 2k_2 e_j)/(e_x + d)$$

Considering the external locally Lipschitz continuous disturbance $\xi(t)$ *as prescribed in the above system:*

$$\dot{\varsigma}_{oj} = G(e_x, e_y)V_o + T(e_x, e_y)V_{jequ} + \xi(t) \tag{23}$$

Assumption 5. *The model uncertainty* ξ *satisfies this condition*

$$sup_t \, \|\xi(t)\| \leq \xi, \exists \forall t \geq 0 \tag{24}$$

where ξ *is the positive semi-definite denoted as* $[\xi_1, \xi_2]^T$. *This assumption facilitates the problem, as relaxing the actual information. This re-formulation assures the finite time transient response using the design of the controller to overcome the uncertainties which are bounded by* ξ. *Under Assumption 5, the formation model in Eq. (21) can be written as:*

$$\dot{\varsigma}_{oj} = T(e_x, e_y)V_{jequ} + \xi \tag{25}$$

$$\dot{\varsigma}_{oj} = G(e_x, e_y)V_o + \tau_{oj} \leq \xi \tag{26}$$

where τ_{oj} *is the disturbance that occurs on the bearing angle. Since* V_o *is the un-measurable velocities of the leader robot, therefore* $G(e_x e_y)V_o$. *As a result, it is regarded as a disturbance.*

Remark 2. The leader–follower tracking model formed in Eq. (26) relies on follower velocities. Moreover, it depends on the changing of saturation and bearing angle distance, which enables us to proceed with the designing of a control scheme without leader information.

https://doi.org/10.1017/S0263574719001772 Published online by Cambridge University Press

4.3. Formation control

In this sub-section, we use a systematic way to design the formation control for NMR. The key idea is to develop a non-singular sliding variable and then decay the error toward zero in finite time with the stable transient response. Let us consider a non-singular continuous terminal sliding surface described as:

$$s(t) = e_{oj}(t) + \frac{1}{\beta_1} e_{oj}(t)^{\frac{g}{h}} + \frac{1}{\beta_2} \dot{e}_{oj}(t)^{\frac{p}{q}} \tag{27}$$

where $e_{oj}(t)$ is the tracking error between the leader and follower, $\beta_1 = \beta_2 > 0$, and p, q, h, g are positive odd integer satisfying this condition $p = q = g = h \geq 0$.

Remark 3. The above sliding surface is non-singular and includes an additional surface for improving the transient response of the system. The fractional power of the terms $e_{oj}^{\frac{g}{h}} = e_{oj}^{\frac{p}{q}}$ is used to increase the convergence rate and keep the system trajectories closed to the sliding surface. In order to obtain the control input v_{jequ}, we set up the sliding surface $s(t) = 0$ define as:

$$s(t) = e_{oj}(t) + \frac{1}{\beta_1} e_{oj}(t)^{\frac{g}{h}} + \frac{1}{\beta_2} \dot{e}_{oj}(t)^{\frac{p}{q}} = 0 \tag{28}$$

Substitute Eqs. (17) and (25) in Eq. (28) to obtain the v_{jequ} equation:

$$V_{jequ} = T(e_x, e_y)^{-1} \left(\left[\beta_2 (e_{oj}(t) + \frac{1}{\beta_1} e_{oj}(t)^{\frac{g}{h}})^{\frac{q}{p}} \right] + \dot{\varsigma}_{oj}^{d} - \xi \right) \tag{29}$$

where $V_{jequ} = [v_j, w_j]$ is used to eliminate the variations, and to ensure the system states are on the sliding surface. The equivalent control is incorporating with the switching control law V_{jswt} as:

$$V_{jsw} = T(ex, ey)^{-1} (K\ sat(s(t))) \tag{30}$$

where K is the switching gain compensation matrix which is used to eliminate the uncertainties from the system. The sat function is used to minimize the chattering phenomena, and ϵ is used to set the boundedness of the system accuracy. The sat(.) function is given as:

$$sat(s(t) = \begin{cases} \frac{s(t)}{\varepsilon} & if \left| \frac{s_k(t)}{\varepsilon} \right| \leq 1 \\ sgn(\frac{s(t}{\varepsilon}) & if \left| \frac{s_k(t)}{\varepsilon} \right| > 1 \end{cases} \quad k = 1, 2$$

The final controller equation can be written as:

$$V_j = T(e_x, e_y)^{-1} \left(\left[\beta_2 (e_{oj}(t) + \frac{1}{\beta_1} e_{oj}(t)^{\frac{g}{h}})^{\frac{q}{p}} \right] + \dot{\varsigma}_{oj}^{d} - \xi + K\ sat(s(t)) \right) \tag{31}$$

Remark 4. The design control Eq. (31) does not contain any singular term. It is faster than the conventional non-singular surface. It provides more accurate tracking and error convergence in the presence of an external disturbance.

Theorem 1. *The proposed control Eq. (31) implemented in the formation model Eq. (31); thus, it surely converges the position error to zero in finite time in the presence of disturbances.*

4.3.1. Stability analysis. According to the lemma.

Lemma 2. *The second-order nonlinear system $\ddot{x} = u$ can be globally uniformly bounded stable under this state feedback control law defined as:*

$$u = -x - \frac{1}{\beta_1} x^{\alpha_1} - \frac{1}{\beta_2} \dot{x}^{\alpha_2}$$

where $\beta_1 = \beta_2 > 0$ and $\alpha_1 \epsilon \left[\frac{g}{h} \right]$, $\alpha_2 = \frac{2\alpha_2}{1 + \alpha_1}$.

https://doi.org/10.1017/S0263574719001772 Published online by Cambridge University Press

Proof: Construct a Lyapunov function as:

$$V = \frac{1}{2} s(t)^T s(t) > 0 \tag{32}$$

Differentiating with respect to s, as a result we get Eq. (33)

$$\dot{V} = s^T(t)\dot{s}(t) \tag{33}$$

taking the differentiation of Eq. (27), we get:

$$\dot{s}(t) = \dot{e}_{oj}(t) + \frac{1}{\beta_1}\frac{g}{h} e_{oj}(t)^{\frac{g}{h}-1}\dot{e}_{oj}(t) + \frac{1}{\beta_2}\frac{p}{q} e_{oj}(t)^{\frac{p}{q}-1}\dot{e}_{oj}(t) \tag{34}$$

substituting Eq. (34) and $\dot{e}_{oj}(t) = (\dot{\varsigma}^d_{oj} - \dot{\varsigma}_{oj})$ and $\dot{\varsigma}_{oj} = T(e_x, e_y)V_j - \xi$ in Eq. (33)

$$\begin{aligned}\dot{V} = s(t)^T \Bigg[\left(\varsigma^d_{oj} - T(e_x e_y)V_j + \xi\right) + \frac{g}{h\beta_1} e(t)^{\frac{g}{h}-1}\left(\dot{\varsigma}^d_{oj} - T(e_x e_y)V_j + \xi\right) + \frac{p}{q\beta_2} e(t)^{\frac{p}{q}-1}\left(\dot{\varsigma}^d_{oj}\right. \\ \left. -T(e_x e_y)V_j + \xi\right) \Bigg]\end{aligned} \tag{35}$$

Substituting the control Eq. (31) into Eq. (35), the new equation defines as:

$$\begin{aligned}\dot{V} = s^T \Bigg[\Bigg[\Bigg(-\beta_2 e(t) - \frac{1}{\beta_1} e(t)^{\frac{g}{h}}\Bigg)^{\frac{q}{p}} - K\, sat(s(t))\Bigg] - \frac{g}{h_{\beta_1}} e(t)^{\frac{g}{h}-1}\Bigg[\Bigg(-\beta_2 e(t) - \frac{1}{\beta_1} e(t)^{\frac{g}{h}}\Bigg)^{\frac{q}{p}} - K\, sat(s(t))\Bigg] \\ - \frac{p}{q_{\beta_2}} e(t)^{\frac{p}{q}-1}\Bigg[\Bigg(-\beta_2 e(t) - \frac{1}{\beta_1} e(t)^{\frac{g}{h}}\Bigg)^{\frac{q}{p}} - K\, sat(s(t))\Bigg]\Bigg]\end{aligned} \tag{36}$$

as the variables $g, h, p, q, \beta_1 = \beta_2 = k[k_1, k_2] > 0$ and $e_{oj}(t)^{\frac{g}{h}-1}, e_{oj}^{\frac{q}{p}-1}$ is converges toward zero. Moreover, due to the negative power of the remaining variables and $(\beta_2 e(t) - \frac{1}{\beta_1} e(t)^{\frac{g}{h}})^{\frac{q}{p}} < K$, then the remaining terms which assure that the system will be stable, and $\dot{V}$ should satisfies this particular condition $\dot{V} \leq 0$ as:

$$\begin{aligned}\dot{V} &= -Ks^T sat(s(t)) \\ \dot{V} &= -K \|s(t)\| \leq 0\end{aligned} \tag{37}$$

From Eq. (37), it is verified that if $s(t) = 0$ then the energy function $\dot{V} \leq 0$ should be negative definite. The system assures to remain on the non-singular sliding surface. Therefore, the position error converges to zero in finite time as $t \to \infty$.

4.3.2. Obstacle avoidance algorithm. Navigating a group of robots, it might be possible to face the obstacle in the path, which is quite a challenging problem. The mapping of the area includes the prior information of the obstacle likely their size and shapes. Therefore, it is very important to incorporate such an obstacle avoidance algorithm to deal with such objects. The algorithm calculates another appropriate path to avoid the collision. Given the robot $[x_j, y_j]$ and the obstacle O_j with position (x_n, y_n). The distance function $\Delta(j, (O_j))$ can be written as:

$$\Delta = \sqrt{\frac{x_j - x_n}{\kappa}^2 + \frac{y_j - y_n}{\kappa}^2} \tag{38}$$

where $\kappa > 0$ is the scaling factor. The obstacle avoidance potential function is described as:

$$\mu_{avoid} = \left(\left\{0, \frac{\Delta^2 - \delta}{\Delta^2 - \delta}\right\}\right)^2 \tag{39}$$

where $\delta, \sigma > 0$ is defined as the radii of detection and avoidance, respectively. The avoidance function Eq. (39) converges to ∞ as a mobile robot reaches the boundary of avoidance, and for the outside

https://doi.org/10.1017/S0263574719001772 Published online by Cambridge University Press

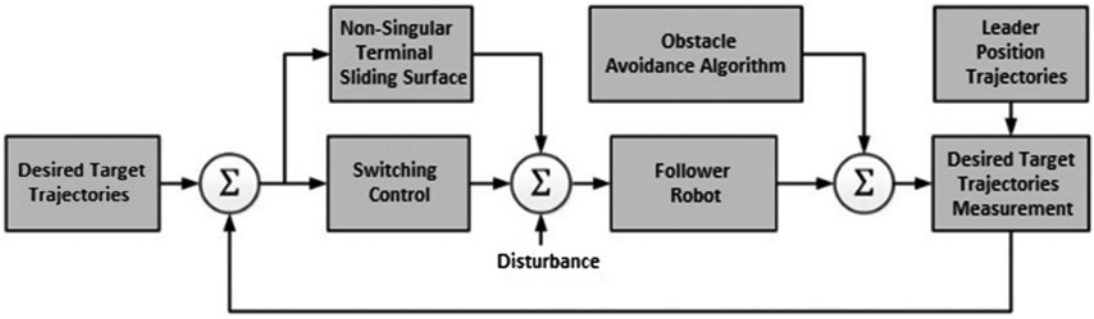


Fig. 12. Block diagram of leader–follower formation control.[2]

of the detection region, it is zero. The function partial derivative concerning Cartesian coordinate is calculated as:

$$\frac{\partial \mu}{\partial x} = \begin{cases} 4\frac{(\delta^2-\sigma_2)(\Delta^2-\delta)}{(\Delta^2-\sigma)^3}(x_j - x_n) & if \delta > \Delta > \sigma \\ 0 & if \sigma > \Delta \geq \delta \end{cases}.$$
$$\frac{\partial \mu}{\partial x} = \begin{cases} 4\frac{(\delta^2-\sigma_2)(\Delta^2-\delta)}{(\Delta^2-\sigma)^3}(y_j - y_n) & if \delta > \Delta > \sigma \\ 0 & if \sigma > \Delta \geq \delta \end{cases}. \tag{40}$$

Therefore, to avoid those objects, the new position vector $\tilde{p}_j$ is defined as:

$$\tilde{p}_j = p_j + p_{obs} = [\tilde{x}_j, \tilde{y}_j, \tilde{\theta}_j]^T$$
$$\tilde{p}_j = \left[x_j + \delta tanh\frac{\partial \mu}{\partial x}, y_j + \delta tanh\frac{\partial \mu}{\partial y}, tan^{-1}\frac{\tilde{\dot{y}}_j}{\tilde{\dot{x}}_j} \right]^T \tag{41}$$

Remark 5. The proposed avoidance algorithm updates the previous position and orientation of the follower robot, when $\delta > \Delta > \sigma$. On the contrary, it remains unchanged when $\sigma > \Delta \geq \delta$. The final control defined in Eq. (31) can maintain the desired pattern between the leader and followers while navigating themselves to perform the desired task. Therefore, no separate algorithm is needed to avoid the obstacle.

4.3.3. Implementation. This sub-section implements the controller on 2 NMRs (one leader and one follower). The overall systematic approach can be seen in Fig. 12. We use curve trajectories as a reference signal.

Curve trajectories. The curve trajectories are obtained by the following equation:

$$v_{jr} = sin(0.008 * \pi * t) + 1, \quad w_{jr} = 0.5sin(0.5 * \pi * t). \tag{42}$$

The control scheme parameters and gains are selected as: $K = [k_1, k_2] = [10, 6]$, $\beta_1 = \beta_2 = 5$, $g = 11$, $h = 3$, $p = 7$, $q = 5$. The desired separation distance and bearing angle are defined as $z^d = [L^d_{oj}, \varphi^d_{oj}] = [1, 240]$. The initial position of each of the robots is set as: $p_o = [1, 1, \pi]$, $p_j = [1, -0.1, 2\pi]$. The external time-varying disturbance is described as: $\xi = \left[\frac{0.01}{2+t} \ \frac{0.01}{1+\frac{1}{t+1}}\right]$.

For simplicity, we assume the communication topology G to be fixed. MATLAB tool is used for simulation, and the subsequent results are shown in Figs. 13, 14, 15, and 16. Figure 13 shows the formation error trajectories converging toward zero. The error converges more quickly as compared to the conventional sliding mode controller. The linear and angular control inputs required to maintain the formation are shown in Fig. 14. Figure 15 shows the entire tracking trajectories using FTSMC. In particular, without considering the leader velocities information and the un-modeled dynamic, the follower robots maintain the desired distance with the leader. Figure 16 shows the NMR trajectories in another pattern, where a follower is continuously tracking the leader by maintaining the estimation distance. The obstacle avoidance algorithm is implemented and is seen in Fig. 17. It shows the NMR

https://doi.org/10.1017/S0263574719001772 Published online by Cambridge University Press

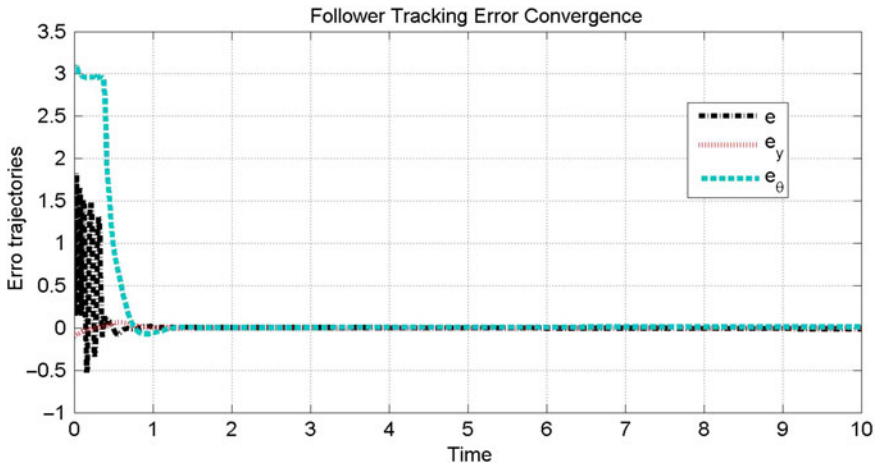


Fig. 13. Follower tracking error convergence.

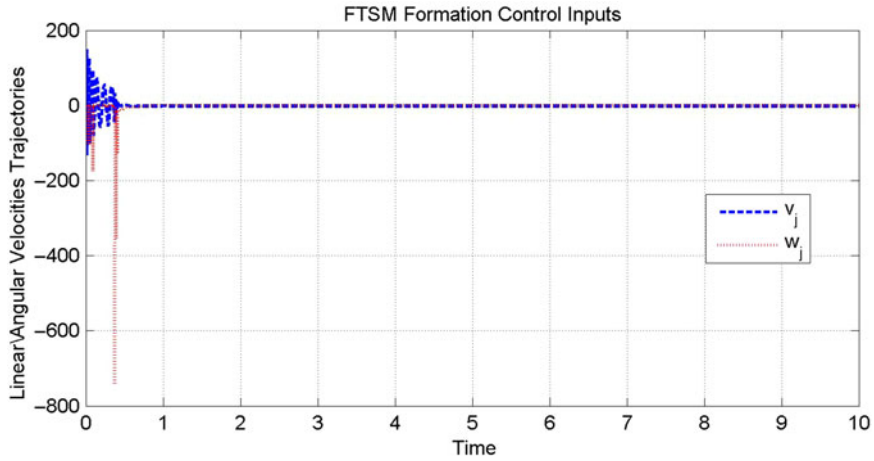


Fig. 14. FTSMC-based formation control inputs.

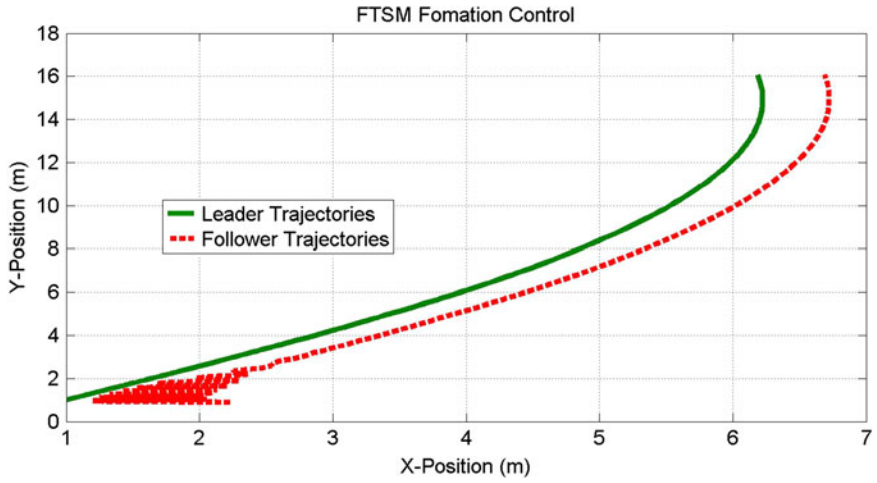


Fig. 15. FTSMC-based NMR trajectories in Cartesian coordinates.

https://doi.org/10.1017/S0263574719001772 Published online by Cambridge University Press

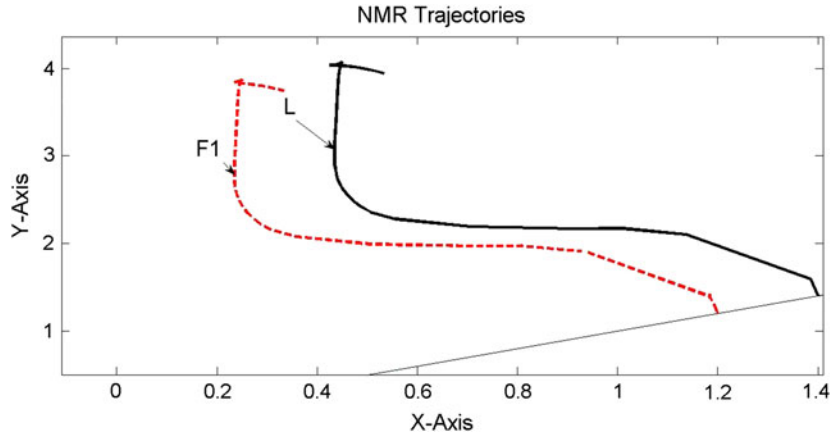


Fig. 16. FTSMC-based NMR trajectories in curve trajectories.

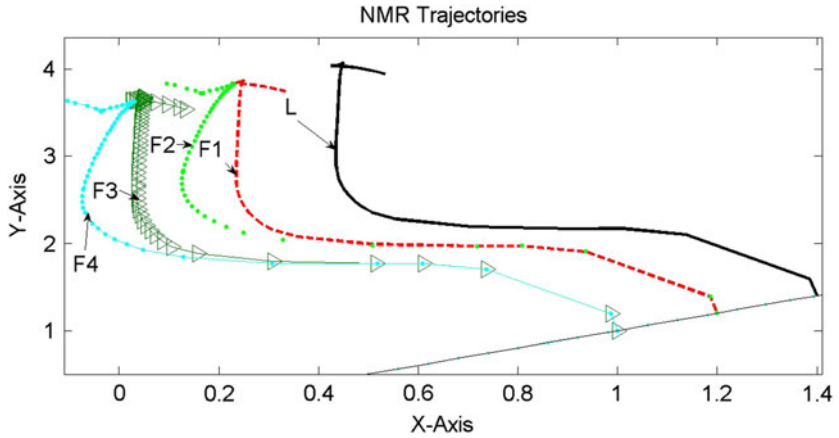


Fig. 17. FTSMC-based four NMR trajectories in curve trajectories.

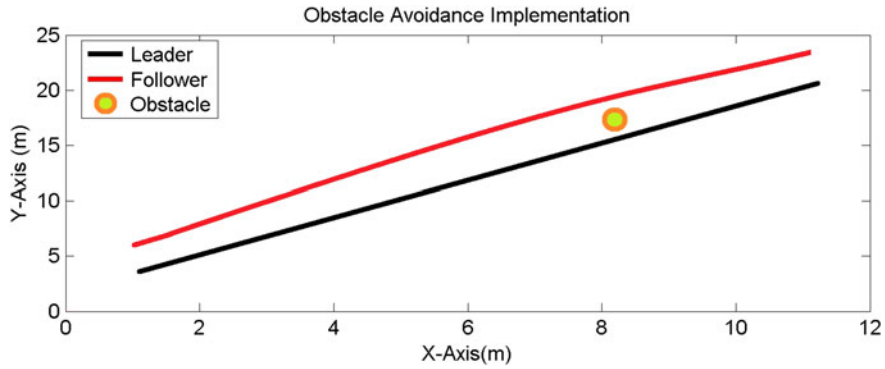


Fig. 18. Implementation of obstacle avoidance algorithm.

trajectories consider four followers. L_1 act as the main leader of the robots, and others are followers. F_1, f_2 also act as the leader for the F_3, F_4 robots, respectively. It ensures the efficacy of the controller and also assures the formation is well established. Figure 18 shows that the follower robot avoids the obstacle and maintains the desired pattern with the leader. The obstacle avoidance algorithm is tested on straight-line trajectories. The FAST non-singular terminal sliding mode control had a better performance, as it was illustrated, the error convergence is only taking 0.85 s. On the other hand, the error convergence rate for conventional sliding mode control was 1.8 or 2.5 s depending on the parameters. There are some fluctuations in the control input signal in conventional SMC, but this method is free from fluctuations. In comparison with other papers, it is more robust and accurate in terms of transient performance, and there are no such singularities in other papers mentioned in the reference.

https://doi.org/10.1017/S0263574719001772 Published online by Cambridge University Press

5. Discussion

In this paper, we proposed a new approach based on fast non-singular sliding mode formation control for a NMR without considering the leader states information. The kinematic model is reformulated as a formation model by incorporating uncertainties and external disturbances. The controller is designed in a two-step process. Firstly, the state-feedback tracking controller is designed. The proposed control achieved the desired objective in a region of interest. The proposed scheme is then extended to output feedback control using high-gain observer. In the second step, the FTSMC controller is designed which ensures the tracking of the leader. The proposed controller ensures high tracking precision. Additionally, an obstacle avoidance algorithm is being incorporated to avoid the collision and improve the system robustness. The effectiveness of the controller is verified and validated using the Lyapunov analysis. All tracking errors converge to zero in finite time, and the closed system is uniformly bounded. Simulation results show the feasibility and efficacy of the desired proposed controller. The first recommendation is to make the system leaderless for an undirected graph. Another recommendation is to design a discrete control in leaderless formation.

References

1. X. Guo, Z. Liang and C. Li, "Finite time tracking control of mobile robot based on non-singular Fast Terminal Sliding Mode," *Syst. Sci. Control Eng.* **6**(1), 492–500 (2018).
2. M. Asif, M. J. Khan and A. Y. Memon, "Integral terminal sliding mode formation control of non-holonomic mobile robots using leader follower approach," *Robotica* **35**(7), 1–15 (2016).
3. L. Zuo, R. Cui and W. Yan, "Terminal sliding mode-based cooperative tracking control for nonlinear dynamic systems," *Trans. Inst. Meas. Control* **52**(2), 1–7 (2016).
4. D. Li and J. Wang, "Nonsingular fast terminal sliding mode control with extended state observer and disturbance compensation for position tracking of electric cylinder," *Math. Prob. Eng.* **2018**, 1–12 (2018).
5. B. M. Yousuf and A. Y. Memon, "Robust Trajectory Tracking Control Design for Nonholonomic Mobile Robot (NMR)," *Proceedings of the 3rd Australia New Zeland Control Conference (ANZCC)*, Melbourne, Australia (2018).
6. N. H. Amer, H. Zamzuri, K. Hudha and Z. A. Kadir, "Modelling and control strategies in path tracking control for autonomous ground vehicles: A review of state of the art and challenges," *J. Intell. Robot. Syst.* **86**(2), 225–254 (2017).
7. M. Cui, D. Sun, W. Liu, M. Zhao and X. Liao, "Adaptive tracking and obstacle avoidance control for mobile robots with unknown sliding," *Int. J. Adv. Robot. Syst.* **9**(171), 1–14 (2012).
8. N. Khalid and A. Y. Memon, "Output Feedback Stabilzation of an Inertia Wheel Pendulum using Sliding Mode Control," *UKACC International Conference on Control*, U.K. (2014), pp. 157–162.
9. M. Defoort, T. Floquet, A. Kokosy and W. Perruquetti, "Sliding-mode formation control for cooperative autonomous mobile robots," *HAL* **55**(11), 3944–3953 (2019).
10. W. Zheng and Y. Jia,"Leader-Follower Formation Control of Mobile Robots with Sliding Mode," *The International Conference on Artificial Life and Robotics (ICAROB)* Seagaia Convention Center, Miyazaki, Japan (2017).
11. E. Lefeber, J. Jakubiak, K. Tchon and H. Nijmeijer, "Observer Based Kinematic Tracking Controllers for a Unicycle-Typoe Mobile Robot," *International Conference on Robotics and Automation,* Seoul Korea (2001), pp. 2084–2089.
12. J. Huang, C. Wen, W. Wang and Z.-P. Jiang, "Adaptive output feedback tracking control of a nonholonomic mobile robot," *Automatica* **50**(3), 821–831 (2014).
13. D. Miklic, S. Bogdan, R. Fierro and Y. Song, "A grid-based approach to formation reconfiguration for a class of robots with non-holonomic constraints," *Eur. J. Control* **18**(2), 162–181 (2012).
14. J. Santiaguillo-Salinas and E. Aranda-Bricaire, "Containment problem with time-varying formation and collision avoidance for multiagent systems," *Int. J. Adv. Robot. Syst.*, 1–13 (2017).
15. X. Chen, Y. Jia and F. Matsuno, "Tracking Control of Nonholonomic Mobile Robots with Velocity and Acceleration Constraints," *American Control Conference*, Portland, OR, USA (2014), 880–884.
16. B. Yousuf, "Robust output feedback formation control for non-holonomic mobile robots (NMRs)," *Robotica* **37**(6), 1–24 (2019).

https://doi.org/10.1017/S0263574719001772 Published online by Cambridge University Press